THE JOURNAL OF PHYSICAL CHEMISTRY B

Article

Cite This: J. Phys. Chem. B 2018, 122, 360−368

pubs.acs.org/JPCB

Influence of the Location of Attractive Polymer−Pore Interactions on Translocation Dynamics

Bappa Ghosh and Srabanti Chaudhury*

Department of Chemistry, Indian Institute of Science Education and Research, Dr. Homi Bhabha Road, Pune 411008, Maharashtra, India

Supporting Information

ABSTRACT: We probe the influence of polymer−pore interactions on the translocation dynamics using Langevin dynamics simulations. We investigate the effect of the strength and location of the polymer−pore interaction using nanopores that are partially charged either at the entry or the exit or on both sides of the pore. We study the change in the translocation time as a function of the strength of the polymer−pore interaction for a given chain length and under the effect of an externally applied field. Under a moderate driving force and a chain length longer than the length of the pore, the translocation time shows a nonmonotonic increase with an increase in the attractive interaction. Also, an interaction on the cis side of the pore can increase the translocation probability. In the presence of an external field and a strong attractive force, the translocation time for shorter chains is independent of the polymer−pore interaction at the entry side of the pore, whereas an interaction on the trans side dominates the translocation process. Our simulation results are rationalized by a qualitative analysis of the free energy landscape for polymer translocation.

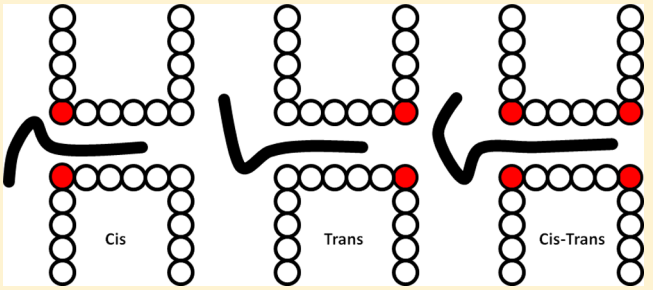

I. INTRODUCTION

The translocation of polymers through a small channel plays an important role in many biological processes such as the transport of DNA and RNA through nuclear pores, the transport of protein through membrane channels,[1] viral injection,[2] and so on. Due to its various potential technological applications such as in gene therapy, DNA sequencing,[3] and drug delivery,[4] polymer translocation has been a subject of a number of experimental,[5,6] theoretical,[7−9] and numerical studies.[10−14] Early in 1996, Kasianowicz et al.[5] and later Berzukov and co-workers[15] have experimentally studied the translocation of single-stranded DNA and RNA molecules through an α-hemolysin channel driven by an external electric field, and the translocation event is monitored by the blockade of the ion channel current. From the theoretical point of view, the translocation process has been modeled as a one-dimensional diffusion problem across a free energy barrier. In such earlier theories, it was considered that unbiased translocation is a quasi-equilibrium process because it was assumed that the translocation time is long enough for the different chain configurations to equilibrate.[7,8] It was later pointed out by Chuang et al.[16] that in the scaling limit, the quasi-equilibrium approximation breaks down at some point. Thus, in polymer translocation, nonequilibrium effects are important[17−19] and need to be taken into account in theory and simulations to capture the proper scaling behavior as observed experimentally.

One of the basic questions in the problem of polymer translocation is the dependence of the translocation time on the system parameters such as the length of polymer chain,[6,10−12,16,20] the length and width of the pore,[10] the secondary structure,[21,22] the salt concentration, the driving force,[6,11,12,20] and the polymer−pore interaction.[21−27] It has been shown experimentally that the translocation of cationic polypeptides can be altered by modifying the distribution of charge in the α-hemolysin pore.[28,29] Two-dimensional (2D) Langevin dynamics simulations by Luo et al. have shown that an attractive interaction can increase the translocation probability, but the average translocation time decreases with an increase in the attractive strength.[23] In most of the earlier studies, it was assumed that the charge density along the pore is constant. Foster et al. have performed two-dimensional molecular dynamics simulations to study the effect of the location of the attractive region on the translocation time for both short and long polymers.[30] Their simulation results are in good qualitative agreement with the experimental findings by Meller et al. on the translocation of a single-stranded DNA through the α-hemolysin pore.[6] Katkar and Muthukumar[26] have performed three-dimensional (3D) Langevin dynamics simulations to study the effect of placing alternate charged and uncharged regions of different lengths along the nanopore on the translocation dynamics of a negatively charged flexible polyelectrolyte passing through a solid-state nanopore[31,32]

Received: September 15, 2017
Revised: December 4, 2017
Published: December 5, 2017

DOI: 10.1021/acs.jpcb.7b09208
J. Phys. Chem. B 2018, 122, 360−368

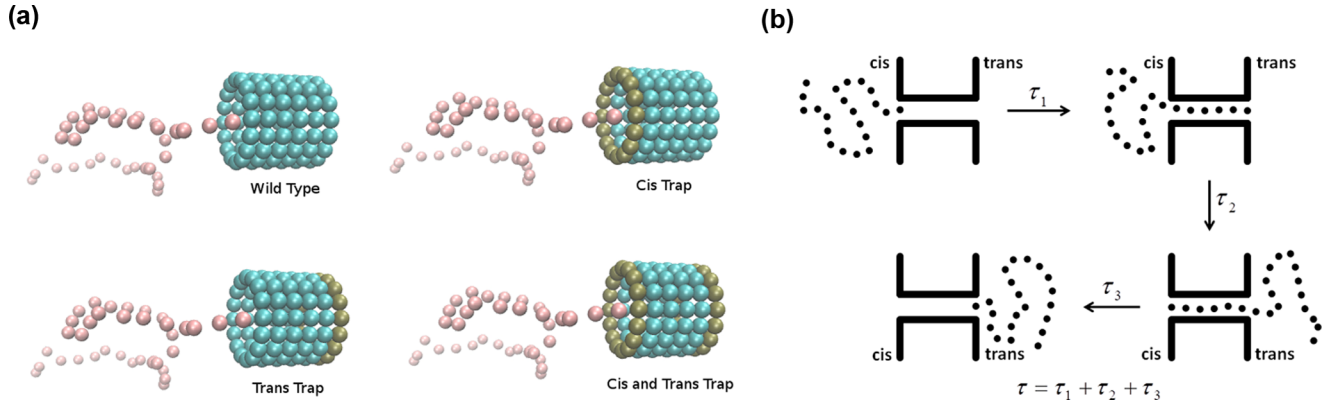

Figure 1. (a) Schematic representation of a polymer chain translocating through a pore of length $L = 6$. (b) Representation of the different components of the total translocation time.

under the influence of a constant electric field. The simulation results are quantitatively supported by a theory based on the Fokker–Planck formalism.[33] Chen et al. have studied the effect of attractive polymer–pore interaction on the translocation dynamics of a polyelectrolyte by performing Monte Carlo simulations with a 2D lattice bond fluctuation model.[25] In this work, we perform three-dimensional Langevin dynamics simulations for the translocation of a charged polymer moving through an interacting channel. We show that the translocation dynamics is strongly influenced not only by the presence of an attractive polymer–pore interaction but also depends on the location of the interaction region. Also, in a recent work by Kolomeisky and Uppulury,[34] a discrete stochastic model was formulated to understand the effect of interaction on the molecular transport across channels and pores. In this model, both the influx and outflux of molecules/ions through biological channel/nanopores were considered. Their results show that molecular transport is accelerated when repulsive interactions are present near the entrance of the pore and attractive interaction is present at the end. Unlike our model, this is a phenomenological random walk model where solvent effects are already taken into account. In our work, we use a coarse-grained description to exclusively study the role of the strength and location of the attractive polymer–pore interaction within the pore in the presence of an external field in the translocation dynamics of the polymer moving from the left to right side of the pore (cis to trans). The details of the simulation are discussed in Section II. In Section III, we discuss the outcome of our simulations, and the obtained results are explained based on the concept of the free energy landscape in Section IV. Finally, we end with our concluding remarks in Section V.

II. SYSTEM

The movement of the polymer chain through a narrow channel is studied by Langevin dynamics simulations using the GROMACS package. The system consists of a membrane, a pore, and a charged polymer chain. The polymer is modeled as a self-avoiding bead–spring chain, with each bead representing a monomer. The beads experience excluded volume interaction, which is given by a short-range repulsive Lennard-Jones (LJ) potential

$$U_{\mathrm{LJ}}(r) = 4\epsilon\left[\left(\frac{\sigma}{r}\right)^{12} - \left(\frac{\sigma}{r}\right)^{6}\right] + \epsilon, \quad \text{if } r \le 1.2\sigma \tag{1a}$$

$$U_{\mathrm{LJ}}(r) = 0, \quad \text{if } r \ge 1.2\sigma \tag{1b}$$

where r is the distance between two monomer beads, ϵ is the interaction strength, and σ is the diameter of the monomer. The consecutive monomer beads are connected by finitely extensible nonlinear elastic (FENE) springs such that

$$U_{\mathrm{FENE}}(r) = -\frac{kR_0^2}{2}\ln\left(1 - \frac{r_{ij}^2}{R_0^2}\right) \tag{2}$$

where k is the FENE spring constant and R_0 is the maximum allowed separation between consecutive monomers. The membrane separating the cis and the trans sides is created by the LJ particles in the yz-plane, with the pore oriented along the x axis. The cylindrical pore is constructed of six consecutive rings of uncharged beads, where each ring consists of 16 monomer beads of diameter σ such that the length of the pore is $L = 6\sigma$ and width $W = 3\sigma$ (Figure 1a). The wall coordinates were frozen during the simulations, and they interact with the polymer chain only via the LJ force. Electrostatic potential between charged beads are modeled by the Coulomb potential

$$U_{\mathrm{int}}(r) = \frac{q_i q_j}{4\pi\epsilon_0 r} \tag{3}$$

where ϵ_0 is the dielectric constant of the medium and q_i and q_j are the charges on the beads i and j that are separated by a distance r. For interaction between polymer beads, $q_1 = q_2$. In most of the previous studies, the electrostatic potential between charged beads is modeled by a truncated Debye–Hückel potential with an exponentially decaying term that contains the Debye length that depends on the concentration of the electrolyte used in the experiments. This is used to screen the electrostatic interaction and reduce the attractive nature of the pore.[35] In our work, this exponentially decaying term is not taken into account as shown in eq 3 to exclusively capture the sole effects of the attraction interactions present within the pore on the translocation dynamics.

In Langevin dynamics simulations, each monomer is subjected to conservative, frictional, and random forces, F_i^{C}, F_i^{F}, and F_i^{R}, respectively.

$$m\ddot{r}_i = -\nabla(U_{\mathrm{LJ}} + U_{\mathrm{FENE}} + U_{\mathrm{int}}) + F_i^{\mathrm{F}} + F_i^{\mathrm{R}} + F_{\mathrm{ext}} \tag{4}$$

where F_i^{F} is the frictional force, $F_i^{\mathrm{F}} = -\eta v_i$, where v_i is the monomer velocity, F_i^{R} is the random force with a zero mean $\langle F_i^{\mathrm{R}}(t)\rangle = 0$, and satisfies the fluctuation–dissipation theorem

DOI: 10.1021/acs.jpcb.7b09208
J. Phys. Chem. B 2018, 122, 360–368

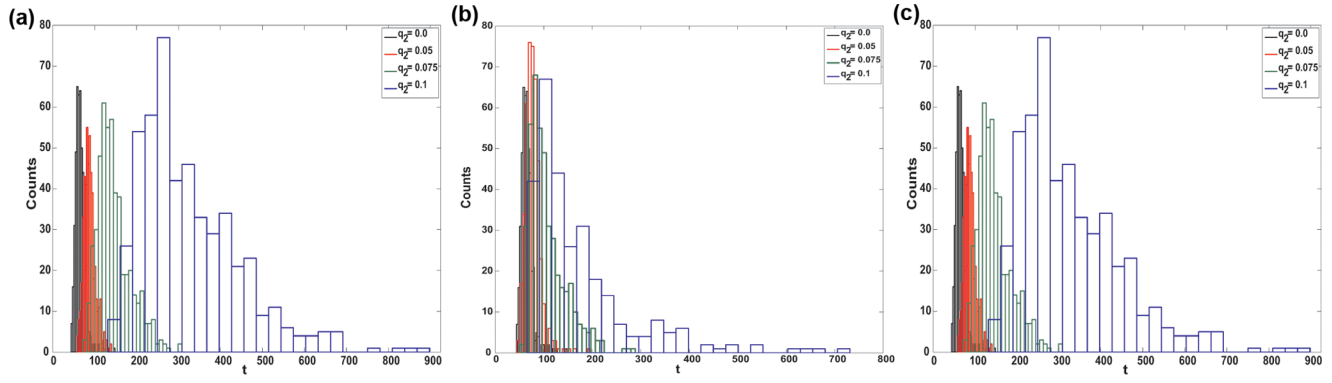

Figure 2. Distribution of translocation time for different attractive strength at (a) cis, (b) trans, (c) cis−trans side of the pore under the driving force of F = 3.3. The length of chain N = 50. q_2 = 0 corresponds to a wild-type pore with no pore−monomer interaction.

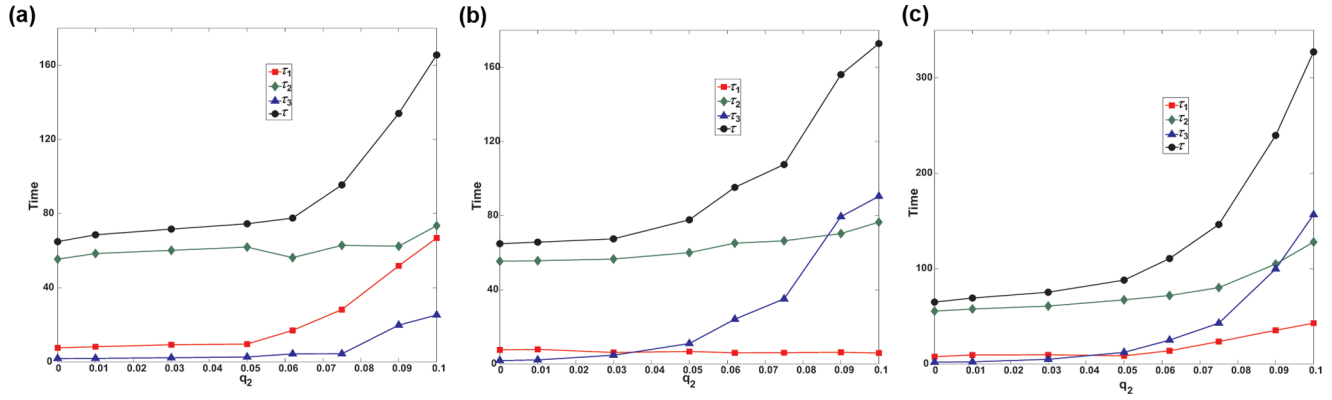

Figure 3. Total translocation time and its components as a function of the attractive strength for interaction at (a) cis, (b) trans, and (c) cis−trans region of the pore under the driving force F = 3.3 and N = 50.

$\langle F_i^R(t)F_j^R(t')\rangle = 6\eta k_B T\delta_{ij}\delta(t-t')$. F_{ext} is the external force due to the electric field, $F_{ext} = F\hat{x}$ where F is the external force acting on the monomers inside the pore and $\hat{x}$ is the unit vector along the axis of the pore. The first monomer is placed at the entrance of the pore and then the polymer is allowed to relax to obtain the equilibrium configuration. The constraint is removed and the whole chain is allowed to evolve according to eq 4 until the chain escapes to the trans side. The integration time step is set to dt = 0.005 units. The results reported in this work are obtained by averaging over 500−1500 independent simulation runs. For each successful translocation event, the translocation time is defined as the time between the entrance of the first bead into the pore from the cis side and the exit of the last monomer bead from the trans side. In the present work, all of the quantities are expressed in dimensionless LJ unit of energy, length, and mass scales. The time scale is defined as $t_{LJ} = \sqrt{\frac{m\epsilon^2}{\sigma}}$. The dimensionless parameters are ϵ_0 = 80, σ = 1, ε = 1, k_BT = 1.2ε, R_0 = 1.5σ, $\xi = \frac{0.7m}{t_{LJ}}$, and $k = 30\frac{\epsilon}{\sigma^2}$. With $\varepsilon_{LJ} = 3.39 \times 10^{-21}$ J, the temperature T = 300 K. The scaling of the driving force of the monomer in the pore is $\frac{\epsilon}{\sigma}$, which is about 3.39 pN.

To study how the location of the interacting region can affect the translocation dynamics, we introduce charges either on the entry side (cis), or the exit side (trans), or both sides (cis and trans) of the pore. To introduce an attractive interaction at the cis side of the pore, a charge of $-q_2e$ is introduced on all of the 16 beads that form the first ring of the pore on the entry side (e = 1.60217646 × 10^{-19} C is the elementary charge). Similarly, interactions on both sides of the pore can be initiated by introducing charges on the beads that form the first and the last ring of the pore. For a given set of parameter values, the translocation time distribution for all of the successful translocation events with attractive interactions at different positions is obtained from which the mean translocation time can be computed and compared.

III. SIMULATION RESULTS

We consider a positively charged polymer chain of N beads, assuming that there are three unit charges per bead and an effective charge for each unit charge is 0.094e. The external driving force F is set between 2.5 and 5 such that it corresponds to the range of voltages used in the experiments. Figure 2 shows the translocation time distribution calculated for a chain of length N = 50 moving from the cis to the trans side of the pore with an attractive interaction placed within the pore at different locations and at an external field strength of F = 3.3. For attractive regions on either the cis, or trans, or both sides of the pore, the histogram of the translocation times deviates from a Gaussian distribution to a long-tailed behavior, with an increase in the value of q_2 thereby leading to a slower translocation. From these distributions, we calculate the first moment, and this corresponds to the mean translocation time, τ. The translocation time of the polymer τ, as defined in the Section I, involves three different time scales, as shown in Figure 1b: τ_1 corresponds to the filling of the pore, τ_2 involves the movement from the cis to trans side of the pore, and τ_3 is

DOI: 10.1021/acs.jpcb.7b09208
J. Phys. Chem. B 2018, 122, 360−368

associated with the emptying of the pore. The mean translocation time τ is a sum of their averages.

Figure 3 shows that the total translocation time τ increases with the increase in q for all of the different types of partially charged pores. For a wild-type pore ($q_2 = 0$), the translocation time depends on the length of the polymer chain N and the strength of the external driving force F (Table 1). Under a moderate driving force of $F = 3.3$ and a long chain of length of $N = 50$, τ initially increases very slowly with increasing q_2 (Table 2). Under the influence of a strong attractive force ($q_2 > 0.05$), the mean translocation time shows a nonmonotonic behavior, with a sharp increase in τ as compared to the case of weak attractive pore interaction placed at either the cis, or trans, or cis−trans region of the pore. Such a scaling behavior as a function of the attractive interaction is same for all of the three conditions of electrostatic traps. We perform simulations to investigate how the three individual time scales τ_1, τ_2, and τ_3 are affected as a function of the polymer−pore interaction q positioned at different locations of the pore. As shown in Figure 3, the position of the attractive region has an impact on the translocation time. Under the effect of strong attractive force on the cis (entry) side of the pore, the mean translocation time τ is dominated by the pore-filling stage, τ_1 (Figure 3a and Table 2a). With a strong attractive interaction on the trans side, τ is determined by the pore-emptying time, τ_3 (Figure 3b and Table 2b). Thus, τ_1 dominates at a strong polymer−pore interaction on the cis side and τ_3 dominates when there is a strong attractive interaction on the trans side of the pore. An attractive force on both the cis and trans sides will affect the pore filling as well as the emptying stage (Table 2c). As a result, a pore with a strong attractive polymer−pore interaction both at the entry and exit sides of the pore will have a maximum effect on the total translocation time τ for a given driving force. The slowest translocation occurs when there is a strong attractive interaction present on both sides of the pore. This is verified when Figure 3c is compared with Figure 3a,b at high values of q_2. These findings are in good agreement with previous experiments and simulations.[21−23] Thus, the distribution of charge along the pore has a significant effect on the mean translocation time.[26,30]

Table 1. Translocation Times for Chain Length N and External Driving Force F Traversing through a Purely Repulsive Pore ($q_2 = 0$)

N	F	τ_1	τ_2	τ_3	$\tau = \tau_1 + \tau_2 + \tau_3$
50	2.5	10.7	72	2.25	85
50	2.9	9.45	64.24	2.13	75.82
50	3.3	7	55.4	1.85	65
50	3.7	6.46	51.62	1.66	59.75
50	4.5	5.57	43.32	1.43	50.32
50	4.8	5.44	39.7	1.3	46.5
35	4.8	5.27	22.32	1.34	28.93
20	4.8	5.39	9.44	1.23	16.06
12	4.8	4.81	4.4	1.25	10.5

Table 2. Translocation Times for Chain Length $N = 50$ and $F = 3.3$ Traversing through a Repulsive Pore with Polymer−Pore Interaction at Different Locations within the Pore

(a) Cis Trap				
q_2	τ_1	τ_2	τ_3	$\tau = \tau_1 + \tau_2 + \tau_3$
0.01	8.2	58.5	1.92	68.6
0.03	9.24	60.2	2.21	71.63
0.05	9.61	61.9	2.63	74.5
0.062	16.99	56.23	4.34	77.58
0.075	28.23	62.9	4.37	95.5
0.09	51.79	62.40	19.81	134.00
0.1	66.85	73.5	26	165
(b) Trans Trap				
q_2	τ_1	τ_2	τ_3	$\tau = \tau_1 + \tau_2 + \tau_3$
0.01	7.9	55.65	2.2	65.7
0.03	6.2	56.6	4.71	67.5
0.05	6.71	60	11	77.8
0.062	6.00	65.14	24.12	95.26
0.075	6.05	66.42	35.1	107.56
0.09	6.29	70.34	79.44	156.08
0.1	5.89	76.5	90.4	172.8
(c) Cis−Trans Trap				
q_2	τ_1	τ_2	τ_3	$\tau = \tau_1 + \tau_2 + \tau_3$
0.01	9.4	57.6	2.2	69.16
0.03	9.63	60.7	4.86	75.2
0.05	8.5	67.24	12.15	87.9
0.062	13.82	71.74	25	110.56
0.075	23.45	80	42.75	146.22
0.09	35.31	104.77	99.57	239.66
0.1	42.75	127.9	156.6	327.3

From our simulations, we can also calculate the translocation probability (P_{trans}), which corresponds to the number of simulation runs that lead to the successful translocation at different positions of the attractive interaction. In case of an unsuccessful translocation, the polymer reverts back to the cis side of the membrane without completing the translocation. The ratio of the number of successful runs to the total number of simulation runs gives the translocation probability, P_{trans}. The translocation probability depends on the strength of the polymer−pore interaction and the magnitude of the applied force. Figure 4a shows P_{trans} as a function of the interaction strength for the case where the polymer experiences an attractive interaction on either the cis side, trans side, or both sides of the pore. Our results show that for a given chain length, when the attractive interaction is present on the cis side of the pore, P_{trans} first increases sharply with the increase in q_2 and becomes saturated at larger values of q_2. When the attraction is on the trans side of the pore, P_{trans} is low and constant. This result supports our intuition that an attraction on the entrance of the pore can facilitate the entry of the chain into the pore. This is same as observed in the translocation of a solute particle across the biological membranes.[36] At the same time, a trans side interaction lowers the probability of the number of translocation runs to be successful. Because the translocation probability is independent of the polymer−pore attraction on the exit side, an interaction on both the cis and trans side affects P_{trans} in a similar manner as observed for an interaction present only at the entrance of the pore. This further supports the fact that an interaction on the trans side of the pore does not increase the translocation probability. Thus, the location of the polymer−pore interaction can alter the frequency of pore entry of the polymer chain. As shown in Figure 4b, the translocation probability increases with the increase in the driving force at a constant q_2. With an increase in the external driving force, the effects of the random thermal noise that is responsible for unsuccessful translocations decrease, as a result of which P_{trans} increases.

DOI: 10.1021/acs.jpcb.7b09208
J. Phys. Chem. B 2018, 122, 360−368

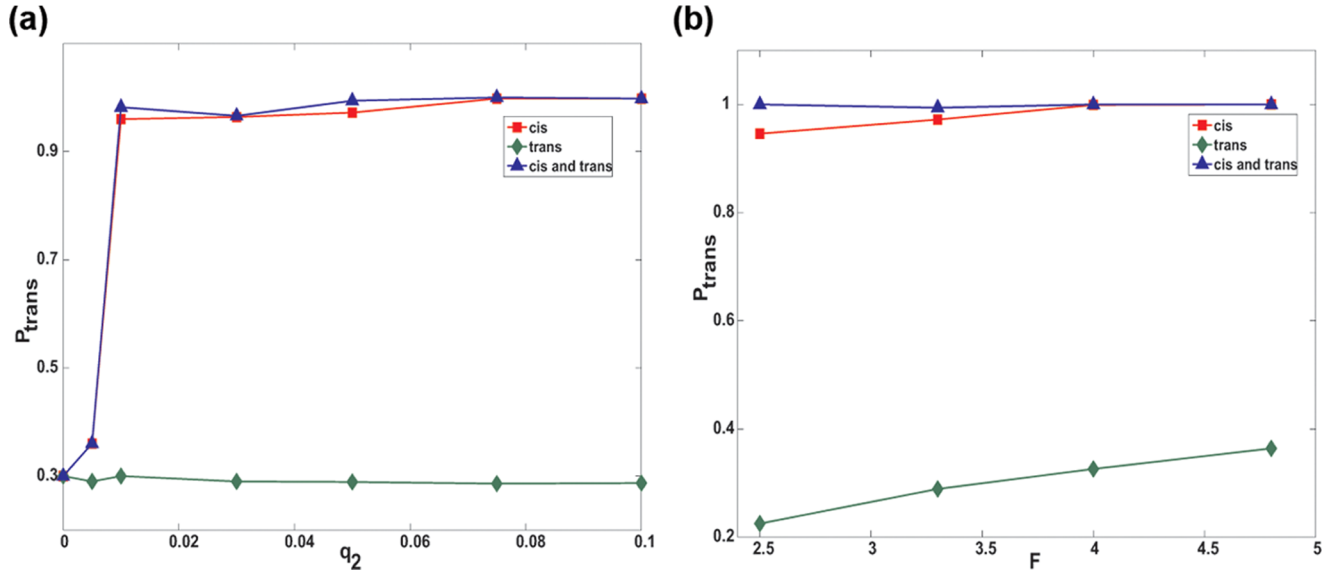

Figure 4. Translocation probability as a function of the (a) attractive strength for interaction at cis, trans, or cis−trans region of the pore under the driving force $F = 3.3$ and $N = 50$ (b) external field strength at $q_2 = 3.3$ and $N = 50$.

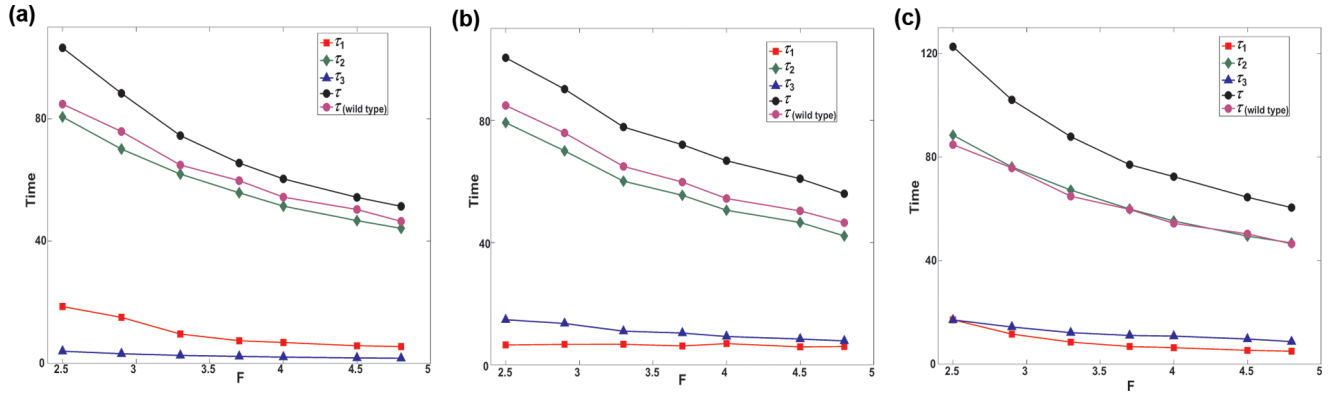

Figure 5. Total translocation time and its components as a function of the driving force for interaction strength $q_2 = 0.05$ at (a) cis, (b) trans, and (c) cis−trans region of the pore with $N = 50$. $q_2 = 0$ corresponds to the wild-type pore.

The dependence of the average translocation time of a polymer chain on the applied electric field at a given polymer−pore interaction positioned at either the cis, or trans, or cis−trans region of the pore is presented in Figure 5. In all of the three cases, the translocation becomes faster with the increase in the strength of the applied field. The translocation time decays nonmonotonically with increase in the applied field. The decay behaviors of the τs' with and without the polymer−pore interaction also suggest that the effect of the polymer−pore interaction is decreased with an increase in the strength of the external electric field. This is evident from the comparison of the translocation time at different driving forces for the wild-type (Table 1) and the partially charged pores (Table 3). The difference between the translocation time of the wild-type and charged pore decreases with an increase in the external driving force (the magenta and the black circles come closer to each other with the increase in F).

Simulations are also performed for shorter chain lengths (N = 12, 20, and 35). In the presence of a strong driving force, F = 4.8, and at moderate to high attractive polymer−pore interaction of $q_2 = 0.05$ and 0.1, respectively, on the cis end of the pore, τ_1 is roughly comparable to that observed for longer chains ($\tau_1^{cis}(N = 12) \approx \tau_1^{cis}(N = 50)$). But τ_2 decreases significantly with a decrease in the chain length (Table 4), thereby decreasing the total translocation time. Thus, τ_1 is independent of the chain length, and the translocation process is dominated by τ_2 for polymer chains of different length but experiencing same attractive interaction on the cis side of the pore. When a strong interaction is present at the trans side, τ_3 is longer for longer chains ($\tau_3^{trans}(N = 12) < \tau_3^{trans}(N = 50)$). For the relatively short chains and strong interaction strength at the exit side or on both sides of the pore, τ_3 increases significantly and has a greater effect on the total translocation time (for N = 12, $\tau_3^{trans}(q = 0.05) \ll \tau_3^{trans}(q = 0.1)$). The translocation time is independent of the presence of attractive polymer−pore interaction on the cis side of the pore.[37]

IV. DISCUSSION

The effect of the translocation time on the strength of the polymer−pore interaction can be explained qualitatively in the context of the free energy landscape.[23,25,30,37−39] In general, this free energy barrier of a polymer translocation event is dependent on the strength of the polymer−pore interaction q,[9,23,39−41] the length of the chain, N,[30] and the strength of the applied external field, F.[8,41] Assuming that polymer translocation is a quasi-equilibrium process, the free energy of the

DOI: 10.1021/acs.jpcb.7b09208
J. Phys. Chem. B 2018, 122, 360−368

Table 3. Translocation Times for Chain Length N = 50 and q_2 = 0.05 at Different Locations within the Pore with Varying Magnitudes of Externally Applied Field

(a) Cis Trap				
F	τ_1	τ_2	τ_3	$\tau = \tau_1 + \tau_2 + \tau_3$
2.5	18.6	80.6	4	103.2
2.9	15.05	70.08	3.17	88.30
3.3	9.61	61.9	2.63	74.5
3.7	7.42	55.79	2.29	65.51
4	6.85	51.42	2.06	60.34
4.5	5.78	46.69	1.81	54.29
4.8	5.51	44.2	1.67	51.36
(b) Trans Trap				
F	τ_1	τ_2	τ_3	$\tau = \tau_1 + \tau_2 + \tau_3$
2.5	6.5	79.2	14.72	100.4
2.9	6.68	70	13.51	90.14
3.3	6.71	60	11	77.8
3.7	6.16	55.42	10.37	71.96
4.0	6.93	50.53	9.26	66.72
4.5	5.86	46.53	8.43	60.84
4.8	6	42.13	7.8	55.93
(c) Cis–Trans Trap				
F	τ_1	τ_2	τ_3	$\tau = \tau_1 + \tau_2 + \tau_3$
2.5	17.1	88.5	17.06	122.7
2.9	11.59	76.2	14.34	102.13
3.3	8.5	67.24	12.15	87.9
3.7	6.79	59.95	11.07	77.07
4	6.33	55.29	10.82	72.43
4.5	5.33	49.45	9.7	64.47
4.8	5	46.8	8.7	60.5

Table 4. Translocation Times for Chain Length N = 12 and F = 4.8 with Polymer–Pore Interaction at Different Locations within the Pore

(a) Cis Trap				
N	τ_1	τ_2	τ_3	$\tau = \tau_1 + \tau_2 + \tau_3$
12 (q_2 = 0.05)	5.69	4.56	1.50	11.75
12 (q_2 = 0.1)	5.40	5	1.89	12.3
20 (q_2 = 0.05)	4.85	10.13	1.60	16.59
35 (q_2 = 0.05)	4.81	23.67	1.73	30.2
50 (q_2 = 0.05)	5.51	44.2	1.67	51.36
(b) Trans Trap				
N	τ_1	τ_2	τ_3	$\tau = \tau_1 + \tau_2 + \tau_3$
12 (q_2 = 0.05)	4.7	4.2	2.06	10.9
12 (q_2 = 0.1)	4.4	4	43.7	56
20 (q_2 = 0.05)	4.59	8.94	7.64	21.2
35 (q_2 = 0.05)	5.1	23.23	7.46	35.8
50 (q_2 = 0.05)	6	42.13	7.8	56
(c) Cis–Trans Trap				
N	τ_1	τ_2	τ_3	$\tau = \tau_1 + \tau_2 + \tau_3$
12 (q_2 = 0.05)	5.75	4.4	2.57	12.72
12 (q_2 = 0.1)	4.4	4.5	64.1	72.89
20 (q_2 = 0.05)	4.64	9.54	9.21	23.29
35 (q_2 = 0.05)	4.53	24.8	7.96	37.39
50 (q_2 = 0.05)	5	46.8	8.7	60.5

polymer is $E = U - TS$, where S is the conformational entropy $S = k_B \ln \Omega$, Ω is the conformational number of the polymer. The internal energy U has two components: (a) the energy U_{int}, which arises due to the polymer–pore electrostatic interaction, and (b) the energy U_{ext} due to the externally applied field F. For a polymer chain that is partially or entirely within the pore, and has a cis trap, the electrostatic interaction energy is given by

$$U_{int}^{cis}(a, b) = \frac{N_r q_1 q_2(1)}{4\pi\epsilon_0} \sum_{i=a}^{b} \frac{1}{r(i, 1)} \tag{5a}$$

where $(b\text{-}a)$ monomers are within the pore, q_1 is the charge on the monomer beads, N_r is the number of pore beads that form the charged ring on the cis side, $q_2(1)$ is the charge on each of these pore beads, and $r(i, 1)$ is the distance between the ith monomer bead and the charged pore ring at the entry side. For a trap at the trans end, the electrostatic interaction energy is given by

$$U_{int}^{trans}(a, b) = \frac{N_r q_1 q_2(L)}{4\pi\epsilon_0} \sum_{i=a}^{b} \frac{1}{r(i, L)} \tag{5b}$$

where $q_2(L)$ is the charge on each of the pore beads on the last ring at the end of the pore and $r(i, L)$ is the distance between the ith monomer bead and the pore ring at the exit side. The contribution to U_{ext} due to the external electric field is given by

$$U_{ext}(a, b) = \sum_{x=a}^{b} Fx \tag{6}$$

The contribution from entropy is given by

$$U_{ent}(n) = k_B T \ln \Omega(n) \tag{7}$$

For n number of monomers at the cis or trans side of the pore, $\Omega(n) = n^{\gamma-1}$, where $\gamma = 0.69$ for a 3D polymer chain. Considering that the part of the chain inside the channel is straight, $\Omega = 1$ for monomers within the pore. The free energy of the polymer is expressed in the unit of $k_B T$. During all of the three stages of translocation, U_{int}, U_{ext}, and U_{ent} will contribute to the free energy of the system, $E = U_{int} + U_{ext} - U_{ent} = U_{int} + U_{ext} + k_B T(1 - \gamma)\ln(n)$. Using the above relations, one can construct the free energy landscape for a translocation coordinate m based on the method described by Katkar and Muthukumar.[26] The contributions of these three different energy terms during the filling, the transfer, and the escape stages with attractive interactions present either on the cis, trans, or both sides of the pore are discussed in the Supporting Information.

To understand the effect of the strength and spatial distribution of the attractive charges, we construct the free energy profile as shown in Figure 6. When a polymer chain enters the pore, there is a decrease in the entropy due to the decrease in the number of available configurations of the chain. For a wild-type pore ($U_{int} = 0$), to enter the pore, the polymer experiences a force due to the external driving force that counterbalances the entropy loss due to confinement. As shown in Figure 6a, a polymer–pore interaction on the cis side of the pore creates a free energy well on the cis side. The polymer chain is trapped inside this well, making it difficult for the chain to fill up the pore ($\tau_1(q_2 = 0) \ll \tau_1^{cis}(q_2 = 0.1)$). The stronger the attraction on the cis side, deeper is the free-energy well and higher is the contribution from U_{int}^{cis} that prevents the polymer from filling the pore. This is also evident from Table 2(a), where a cis trap increases τ_1. During the transfer stage, there is a balance between the external driving force and the opposing force due to attractive attraction with the pore. In the escape stage, the external driving force and the entropy gain due to

DOI: 10.1021/acs.jpcb.7b09208
J. Phys. Chem. B 2018, 122, 360–368

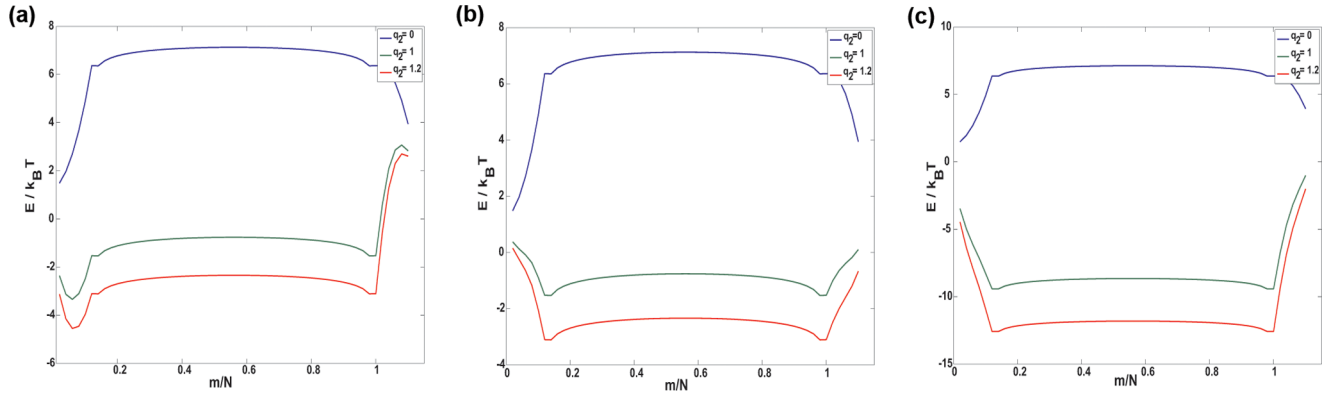

Figure 6. Free energy landscape for a polymer chain of length $N = 50$ translocating through a nanopore of length $L = 6$ with different attractive strengths at (a) cis, (b) trans, and (c) cis−trans region of the pore under the driving force $F = 0.3$.

deconfinement need to overcome this interaction energy for the polymer to escape from the pore. Because the effect of the attractive charges present on the cis side is weak during the pore-emptying stage, it does not show any significant effect on the pore-emptying time. Hence, the free energy profile at the end of the pore does not change with the change in the strength of the cis attraction, as shown in Figure 6a. In Figure 6b, we find that a trans trap creates a wide free energy well for the translocation that prevents the polymer to escape from the pore ($\tau_3^{\text{trans}}(q_2 = 0) \ll \tau_3^{\text{trans}}(q_2 = 0.1)$). A stronger interaction on the trans side increases the depth of this free energy well (contribution from $U_{\text{int}}^{\text{trans}}$ increases, Figure 6b). During the pore-emptying stage, only a few monomers are present inside the pore and U_{ext} goes on decreasing. Because charges are present near the pore end, the attractive force felt near the pore end increases. The electric driving force is insufficient to overcome this attractive force $U_{\text{int}}^{\text{trans}}$ and causes the trapping of the polymer within the pore, thereby increasing τ_3. When traps are present on both ends of the pore, for a given attractive strength, the free energy well is more negative, indicating that the effect of the attractive interactions increases (Figure 6c; $\tau^{\text{trans}}(q_2, N) < \tau^{\text{cis-trans}}(q_2, N)$, as seen in Table 2b,c). In this case, the polymer first overcomes the free energy on the cis side and fills up the pore. During the transfer stage, the tail part of the chain that was outside the pore enters the pore and the head monomeric part leaves the pore from the trans side. The presence of trans trap attracts the positively charged monomers confined within the pore toward the pore end; also, the number of monomer beads within the pore is small, U_{ext} goes on decreasing. Because there is no external driving force acting on the monomer beads that have already translocated through the pore, these beads are also attracted toward the trans trap, thereby causing crowding near the pore end.[30] This crowding effect affects the monomers confined within the pore and the monomers that are near the pore exit. Thus, in the emptying stage, there is a significant trapping of the polymer at the trans end of the pore. This indicates that the effect of an attractive electrostatic interaction on the trans side is high compared to that on the cis side if all of the other parameters are kept fixed. As shown in Figure 6c, the free energy cost during the filling stage is less than the free energy cost during the emptying stage. This intuition is also supported by our simulation results. For a given chain length and with attractive interactions present on both sides of the pore, the increase in translocation time due to the trans side trap is more compared to that due to the cis side trap ($\tau_1^{\text{cis-trans}}(q_2, N) < \tau_3^{\text{cis-trans}}(q_2, N)$; Table 2c).

We find that the free energy landscape in Figure 6 estimated from the equation $E = U - TS$ shows three different behaviors that are also observed in our Langevin dynamics simulations. Thus, our theoretical calculations of the free energy profile provide a satisfactory qualitative explanation of our simulation results on the effect of the strength and spatial distribution of the attractive charges along the nanopore. Quantitative comparison between the theoretical and numerical results is not possible because the formula used for estimating the free energy theoretically is valid in the quasi-equilibrium assumption, but polymer translocation is an out-of-equilibrium process that can be adequately captured only in our simulations. Also, the crowding effect at the trans end of the pore is not accounted for in the free energy calculations. As shown in Figure 6, the free energy calculations are done at charges $q_2 = 1$, 1.2, and external force ($F = 0.3$) to capture the contributions of τ_1, τ_2, and τ_3 to the mean translocation time in the presence of attractive interactions positioned at different regions of the pore. It is very difficult to simulate the translocation of a polymer at such high values of q_2 and low values *of* F; the simulations will be extremely slow. From the free energy landscape, one can also use the Fokker−Planck formalism to theoretically calculate the translocation time of the polymer by assuming a position-independent diffusion coefficient.[42] But again, there will be disagreement between the theoretical and simulation methods due to the quasi-equilibrium assumption in the Fokker−Planck equation. The position-dependent and interaction-dependent diffusion properties that are neglected in the theoretical calculations of the translocation time are included in our simulations.

The free energy landscape is also dependent on the strength of the driving force F. A stronger driving force can tilt the landscape and can make the translocation process faster.[39] Though an attractive polymer−pore interaction at either or both ends of the pore causes trapping of the polymer inside the pore, increasing the strength of the applied voltage facilitates the translocation process (at $q_2 = 0.05$, $\tau^{\text{cis,trans,cis-trans}}(F = 3.3) > \tau^{\text{cis,trans,cis-trans}}(F = 4.8)$). As a result, with an increase in the external driving force, the effect of the polymer−pore interaction decreases. For chain lengths longer than the length of the pore ($N = 12$, 20, 35, and 50), the filling time τ_1 is almost constant. This is because, during the filling stage, the numbers of monomers confined within the pore is roughly the same for all of the chain lengths. This number corresponds to the maximum number of monomers that can be accommodated within the pore. Thus, the presence of a cis trap does not

DOI: 10.1021/acs.jpcb.7b09208
J. Phys. Chem. B 2018, 122, 360−368

influence τ_1 for chains of different length (Table 4a). During the transfer stage, the last polymer bead needs to reach the cis end of the pore. This process is longer for chains of longer length, hence τ_2 increases with increase in the chain length. When the trap is at the trans end, the crowding effect felt by the monomers confined within the pore is same for both chain lengths. But for smaller chains, there are less number of monomer beads that are already on the trans side and are attracted toward the pore wall. Hence, it is easier to overcome the free energy cost during the emptying stage for short chains. Thus, τ_3 increases with increase in chain length, as reported in Table 4b.

Experiments have shown that the translocation time of a polymer can be tuned by introducing the polymer−pore interaction. Mohammad et al.[28] have experimentally studied the effect of polymer−pore interaction at the single molecule level. The presence of electrostatic traps on both sides the pore leads to longer times of current blockade (the residence probability is increased) when compared to the wild-type pore or a pore with attractive interaction at either end (wild type < entry trap < exit trap < entry and exit trap). This is in agreement with our numerical simulation results where we find that the translocation times are increased when traps are present on both ends of the pore. Wolfe et al. have shown that electrostatic traps positioned at definite positions within the pore can facilitate the translocation of a polymer.[29] But these experiments are quite complicated where one needs to take care of the hydrophobicity of the polypeptide, the polypeptide sequence, the ionic strength of the aqueous phase, and the transmembrane potential; all of which have not been explicitly taken into account in our numerical simulations. Hence, it is not possible to relate our simulations results directly to such an experimental setup. Our model is a coarse-grained picture where we intend to capture the sole effects of the polymer−pore interaction in the translocation of the polymer from one side of the membrane to other.

V. CONCLUSIONS

To summarize, in this article, we investigate the role of attractive polymer interaction in the translocation process and show that the location of the polymer−pore interaction plays a crucial role in the pore-driven translocation of a charged polymer chain. The position of the electrostatic interaction causes variation in the dependence of the total translocation time as a function of the attractive interaction strength, the external field, and the chain length. For a given chain length and in the presence of an externally applied field, the translocation time τ, which is composed of three different time scales τ_1, τ_2, and τ_3, increases nonmonotonically with an increase in the polymer−pore interaction. The position of the interaction region causes changes in the dependence of the translocation time on the strength of the polymer−pore interaction. With the increase in the attractive strength on the cis side of the pore, τ_1 contributes dominantly to τ, whereas τ is determined by τ_3 when the interaction is on the trans side. The translocation is slowest when a strong polymer−pore interaction is present on both sides of the pore. We have shown that the effect of the polymer−pore interaction decreases with increase in the strength of the external field. Under a strong attractive force, and for shorter polymer chains, the dependence of the translocation time on the strength and location of attractive polymer−pore interaction is different. From our simulation results, we can conclude that a strong polymer−pore interaction introduced on the exit side or both sides of the pore governs the translocation time for shorter chains, whereas an interaction on the entry side has no significant effect. Also, for chains of different length, the translocation time at the given external field strength and with attractive interactions at specific regions of the pore is dominated by τ_2. The decrease in the translocation time with the decrease in the length of the chain is mainly due to the decrease in τ_2.

The effect of polymer−pore interaction on the translocation of a polymer is explained by constructing the free energy landscape of polymer translocation. In our work, the different behaviors of the polymer translocation process under the influence of polymer−pore interaction are explained qualitatively by analyzing the contribution of the different energy terms in the equation for the free energy of the polymer. Polymer translocation is essentially an out-of-equilibrium process, which is a big challenge for theoretical calculations. Our simulations provide an important tool to capture the nonequilibrium dynamics and understand the polymer translocation in the presence of attractive polymer−pore interactions. In governing the translocation time, incorporation of an electrostatic attractive trap on the trans end of the pore can be more effective compared to the cis trap. Our conclusions are based on a coarse-grained description of the translocation dynamics by explicitly considering the individual contributions of the filling, transfer, and escape stage to the translocation time, which is difficult to obtain from the experiments. Our results show that the translocation dynamics can be modified and tuned by altering the strength and spatial distributions of the attractive polymer−pore interaction.

■ ASSOCIATED CONTENT

Supporting Information

The Supporting Information is available free of charge on the ACS Publications website at DOI: 10.1021/acs.jpcb.7b09208.

Calculation of free energy for translocation with attractive interaction at cis, or trans, or cis−trans region of the pore (PDF)

■ AUTHOR INFORMATION

Corresponding Author

*E-mail: srabanti@iiserpune.ac.in. Phone: 912025908140.

ORCID

Srabanti Chaudhury: 0000-0001-6718-8886

Notes

The authors declare no competing financial interest.

■ ACKNOWLEDGMENTS

The authors would like to acknowledge DAE-BRNS (37(2)/14/08/2016-BRNS/37022) and IISER Pune for funding. B.G. thanks IISER Pune for fellowship. The authors acknowledge C-DAC Pune for computational facilities.

■ REFERENCES

(1) Akeson, M.; Branton, D.; Kasianowicz, J. J.; Brandin, E.; Deamer, D. W. Microsecond Time-Scale Discrimination among Polycytidylic Acid, Polyadenylic Acid, and Polyuridylic Acid as Homopolymers or as Segments within Single RNA Molecules. *Biophys. J.* **1999**, *77*, 3227−3233.

(2) Lingappa, V. R.; Chaidez, J.; Yost, C. S.; Hedgpeth, J. Determinants for Protein Localization: Beta-Lactamase Signal

Sequence Directs Globin across Microsomal Membranes. *Proc. Natl Acad. Sci. U.S.A.* **1984**, *81*, 456−460.
(3) Turner, S. W. P.; Cabodi, M.; Craighead, H. G. Confinement-Induced Entropic Recoil of Single DNA Molecules in a Nanofluidic Structure. *Phys. Rev. Lett.* **2002**, *88*, 128103.
(4) Chang, D. C. *Guide to Electroporation and Electrofusion*; Academic Press: New York, 1992.
(5) Kasianowicz, J. J.; Brandin, E.; Branton, D.; Deamer, D. W. Characterization of Individual Polynucleotide Molecules Using a Membrane Channel. *Proc. Natl. Acad. Sci. U.S.A.* **1996**, *93*, 13770−13773.
(6) Meller, A.; Nivon, L.; Branton, D. Voltage-Driven DNA Translocations through a Nanopore. *Phys. Rev. Lett.* **2001**, *86*, 3435.
(7) Sung, W.; Park, P. J. Polymer Translocation through a Pore in a Membrane. *Phys. Rev. Lett.* **1996**, *77*, 783.
(8) Muthukumar, M. Polymer Translocation through a Hole. *J. Chem. Phys.* **1999**, *111*, 10371.
(9) Muthukumar, M. Polymer Escape through a Nanopore. *J. Chem. Phys.* **2003**, *118*, 5174.
(10) Luo, K.; Ala-Nissila, T.; Ying, S.-C. Polymer Translocation through a Nanopore: A Two-Dimensional Monte Carlo Study. *J. Chem. Phys.* **2006**, *124*, 034714.
(11) Tian, P.; Smith, G. D. Translocation of a Polymer Chain across a Nanopore: A Brownian Dynamics Simulation Study. *J. Chem. Phys.* **2003**, *119*, 11475.
(12) Luo, K.; Huopaniemi, I.; Ala-Nissila, T.; Ying, S.-C. Polymer Translocation through a Nanopore under an Applied External Field. *J. Chem. Phys.* **2006**, *124*, 114704.
(13) Panja, D.; Barkema, G. T.; Ball, R. C. Anomalous Dynamics of Unbiased Polymer Translocation through a Narrow Pore. *J. Phys.: Condens. Matter* **2007**, *19*, 432202.
(14) Vocks, H.; Panja, D.; Barkema, G. T.; Ball, R. C. Pore-Blockade Times for Field-Driven Polymer Translocation. *J. Phys.: Condens. Matter* **2008**, *20*, 095224.
(15) Bezrukov, S. M.; Vodyanoy, I.; Brutyan, R. A.; Kasianowicz, J. J. Dynamics and Free Energy of Polymers Partitioning into a Nanoscale Pore. *Macromolecules* **1996**, *29*, 8517−8522.
(16) Chuang, J.; Kantor, Y.; Kardar, M. Anomalous Dynamics of Translocation. *Phys. Rev. E* **2001**, *65*, 011802.
(17) Luo, K.; Ala-Nissila, T.; Ying, S.-C.; Metzler, R. Driven Polymer Translocation through Nanopores: Slow-Vs.-Fast Dynamics. *Europhys. Lett.* **2009**, *88*, 68006.
(18) Lehtola, V. V.; Linna, R. P.; Kaski, K. Dynamics of Forced Biopolymer Translocation. *Europhys. Lett.* **2009**, *85*, 58006.
(19) Panja, D.; Barkema, G. T.; Kolomeisky, A. B. Through the Eye of the Needle: Recent Advances in Understanding Biopolymer Translocation. *J. Phys.: Condens. Matter* **2013**, *25*, 413101.
(20) Ikonen, T.; Bhattacharya, A.; Ala-Nissila, T.; Sung, W. Influence of Non-Universal Effects on Dynamical Scaling in Driven Polymer Translocation. *J. Chem. Phys.* **2012**, *137*, 085101.
(21) Meller, A.; Nivon, L.; Brandin, E.; Golovchenko, J.; Branton, D. Rapid Nanopore Discrimination between Single Polynucleotide Molecules. *Proc. Natl. Acad. Sci. U.S.A.* **2000**, *97*, 1079−1084.
(22) Meller, A.; Branton, D. Single Molecule Measurements of DNA Transport through a Nanopore. *Electrophoresis* **2002**, *23*, 2583−2591.
(23) Luo, K.; Ala-Nissila, T.; Ying, S.-C.; Bhattacharya, A. Influence of Polymer−Pore Interactions on Translocation. *Phys. Rev. Lett.* **2007**, *99*, 148102.
(24) Mirigian, S.; Wang, Y.; Muthukumar, M. Translocation of a Heterogeneous Polymer. *J. Chem. Phys.* **2012**, *137*, 064904.
(25) Chen, Y.-C.; Wang, C.; Zhou, Y.-L.; Luo, M.-B. Effect of Attractive Polymer−Pore Interactions on Translocation Dynamics. *J. Chem. Phys.* **2009**, *130*, 054902.
(26) Katkar, H. H.; Muthukumar, M. Effect of Charge Patterns Along a Solid-State Nanopore on Polyelectrolyte Translocation. *J. Chem. Phys.* **2014**, *140*, 135102.
(27) Mohan, A.; Kolomeisky, A. B.; Pasquali, M. Effect of Charge Distribution on the Translocation of an Inhomogeneously Charged Polymer through a Nanopore. *J. Chem. Phys.* **2008**, *128*, 125104.
(28) Mohammad, M. M.; Prakash, S.; Matouschek, A.; Movileanu, L. Controlling a Single Protein in a Nanopore through Electrostatic Traps. *J. Am. Chem. Soc.* **2008**, *130*, 4081−4088.
(29) Wolfe, A. J.; Mohammad, M. M.; Cheley, S.; Bayley, H.; Movileanu, L. Catalyzing the Translocation of Polypeptides through Attractive Interactions. *J. Am. Chem. Soc.* **2007**, *129*, 14034−14041.
(30) Piguet, F.; Foster, D. P. Translocation of Short and Long Polymers through an Interacting Pore. *J. Chem. Phys.* **2013**, *138*, 084902.
(31) Chen, P.; Gu, J.; Brandin, E.; Kim, Y.-R.; Wang, Q.; Branton, D. Probing Single DNA Molecule Transport Using Fabricated Nanopores. *Nano Lett.* **2004**, *4*, 2293−2298.
(32) Kowalczyk, S. W.; Wells, D. B.; Aksimentiev, A.; Dekker, C. Slowing Down DNA Translocation through a Nanopore in Lithium Chloride. *Nano Lett.* **2012**, *12*, 1038−1044.
(33) Muthukumar, M. *Polymer Translocation*; Taylor & Francis: Boca Raton, 2011.
(34) Kolomeisky, A. B.; Uppulury, K. How Interactions Control Molecular Transport in Channels. *J. Stat. Phys.* **2011**, *142*, 1268−1276.
(35) Oukhaled, G.; Bacri, L.; Mathé, J.; Pelta, J.; Auvray, L. Effect of Screening on the Transport of Polyelectrolytes through Nanopores. *Europhys. Lett.* **2008**, *82*, 48003.
(36) Berezhkovskii, A. M.; Pustovoit, M. A.; Bezrukov, S. M. Channel-Facilitated Membrane Transport: Transit Probability and Interaction with the Channel. *J. Chem. Phys.* **2002**, *116*, 9952.
(37) Sun, L.-Z.; Luo, M.-B. Langevin Dynamics Simulation on the Translocation of Polymer through α-Hemolysin Pore. *J. Phys.: Condens. Matter* **2014**, *26*, 415101.
(38) Luo, K.; Ala-Nissila, T.; Ying, S.-C.; Bhattacharya, A. Translocation Dynamics with Attractive Nanopore−Polymer Interactions. *Phys. Rev. E* **2008**, *78*, 061918.
(39) Luo, M.-B.; Cao, W.-P. Influence of Polymer−Pore Interaction on the Translocation of a Polymer through a Nanopore. *Phys. Rev. E* **2012**, *86*, 031914.
(40) Sun, L.-Z.; Cao, W.-P.; Luo, M.-B. Free Energy Landscape for the Translocation of Polymer through an Interacting Pore. *J. Chem. Phys.* **2009**, *131*, 194904.
(41) Wang, C.; Chen, Y.-C.; Zhou, Y.-L.; Luo, M.-B. Escape of Polymer Chains from an Attractive Channel under Electrical Force. *J. Chem. Phys.* **2011**, *134*, 064905.
(42) Zhang, S.; Wang, C.; Sun, L.-Z.; Li, C.-Y.; Luo, M.-B. Polymer Translocation through a Gradient Channel. *J. Chem. Phys.* **2013**, *139*, 044902.

DOI: 10.1021/acs.jpcb.7b09208
J. Phys. Chem. B 2018, 122, 360−368